

MRI Detection of Glycogen (GlycoCEST)

C. K. Jones^{1,2}, J. Ren³, C. Malloy³, A. D. Sherry³, P. C. van Zijl^{1,2}

¹F.M. Kirby Center for Functional Brain Imaging, Kennedy Krieger Institute, Baltimore, MD, United States, ²Dept of Radiology and Radiological Sciences, Johns Hopkins University School of Medicine, Baltimore, MD, United States, ³Advanced Imaging Research Center, University of Texas Southwestern Medical Center, Dallas, TX, United States

Introduction: The importance of glycogen in carbohydrate metabolism of the liver, heart, and skeletal muscle is widely appreciated. Abnormalities of glycogen metabolism are central to some rare inherited disorders, but glycogen metabolism may also be abnormal in very common medical conditions such as insulin resistance and Type-2 diabetes (T2D). Much of this information has been developed from animal studies or relatively indirect measurements in human subjects or a small number of invasive studies. Defining the role of glycogen is important for understanding the pathophysiology of these diseases. The only noninvasive approach to glycogen content *in vivo* is MR spectroscopy (MRS), allowing direct measurement of glycogen concentration by detecting natural abundance ¹³C in carbon-1 of glycogen. However, these methods are available only in specialized research sites. Quantification of glycogen content in liver and other organs would be useful for a variety of applications if it could be performed with standard MRI. We show that this is possible using selective radiofrequency saturation of the hydroxyl protons. This saturation is rapidly transferred to the water protons via chemical exchange, leading to a cumulative saturation of the water signal and enhanced glycogen detection sensitivity via the so-called chemical exchange saturation transfer (CEST) mechanism (1). We here demonstrate this "GlycoCEST" effect in the perfused liver following alternate perfusion with glucose-rich medium and with glucose-free medium with glucagon

Methods: Healthy female mice, strain C57BL6 (22±2g), were provided continuous access to food. Mice were anesthetized by i.m. injection of ketamine prior to a mid-line laparotomy to expose the liver. The portal vein was cannulated and immediately perfused (8mL/min) with Krebs-Henseleit (KH) buffer containing heparin. The hepatic vein and inferior vena cava were dissected, and the liver was carefully removed and placed in a container positioned directly above a 2.5 cm ¹H surface coil. Livers were perfused with KH buffer containing 10mM glucose (Glc) during isolation and MRS setup. Subsequently, the perfusate was switched to glucose-free KH buffer so that effluent perfusate samples could be analyzed for glucose coming from the liver. A solution of glucagon (500pg/mL) was prepared fresh in KH buffer containing BSA and MRI was performed during perfusion with this solution. MTR images as a function of offset frequency with respect to water were collected at 4.7T (±1.5ppm) and MTRasym = {MTR(-1.5ppm) - MTR(1.5ppm)}/MTR(-1.5ppm) was calculated for the primary liver lobe regions. In a separate experiment, 1H-decoupled ¹³C spectroscopy and MTRasym measurements were compared at 9.4T.

Results: Fig. 1 shows a baseline MT image of a fed mouse liver (black liver, bright perfusate) at 1.5ppm offset from water, and colored MTRasym images as a function of time after initiating the glucagon perfusion. The graphs show changes in [Glc] and MTRasym, which correlate well. The declining MTRasym (relative intensity) during the 90 min glucagon perfusion was indicative of decreasing hepatic glycogen storage due to glucagon-induced glycogen depletion, which is consistent with the continuously decreasing hepatic glucose disposal to the perfusion. Fig. 2 shows MTRasym spectra and corresponding ¹H-decoupled ¹³C spectra at 9.4T, confirming that glycogen was present and decreased after glucagon. The relative area of the MTRasym (from 0-1.5ppm) and of glycogen C1 with and without glucagon perfusion were 2.5 and 4.5, respectively.

Discussion and Conclusion: Hepatic glycogen can be detected using a simple GlycoCEST experiment. Further experiments will need to be done for a calibration of the glycogen MTRasym as a function of glycogen concentration as measured by ¹³C spectroscopy. Extension to humans would allow non-invasive imaging of glycogen in a series of disorders. Such imaging will be easier at higher magnetic fields as the glycogen hydroxyl protons will be better separated from water.

References: 1) Ward KM, et al., JMR 2000;143:79-87. 2) Roden, M, et al., Rec. Progr. Horm. Res. 2001, 56 :219-237. Grant support: NIH NCRR (RR-02584); NIH (CA-84697); Robert A. Welch Foundation (AT-584); Philips Medical Systems.

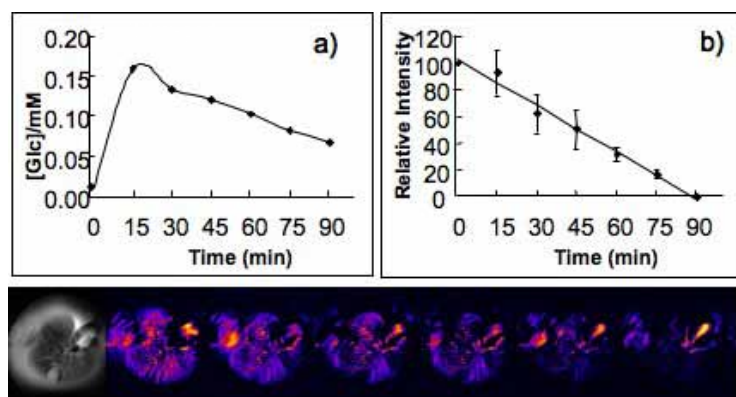


Fig. 1: Glucagon effect on glycogen imaging of a perfused fed-mouse liver at 4.7T (37°C). The black image at t=0 marks the beginning of perfusion with glucose-free media containing 500 pg/ml glucagon. Color images represent MTRasym for irradiation at ±1.5 ppm (length 1s, 60 Hz power) from water, a) glucose concentration in effluent perfusate vs time; b) MTRasym vs time, representing the declining liver glycogen storage. Intensity was scaled to 100 for t=0 and to 0 for t=90 mins.

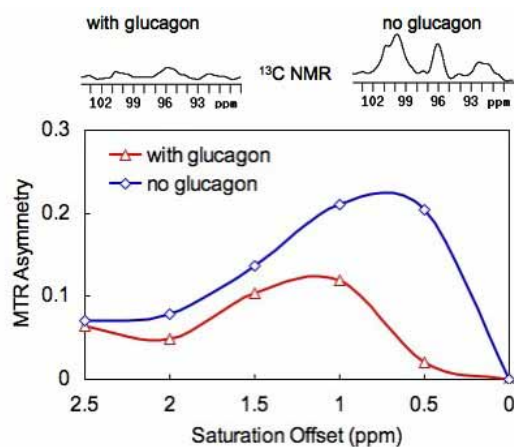


Fig 2: Comparison of GlycoCEST and ¹³C MRS in sliced fed liver at 9.4T (21°C). No glucagon: perfusion with 10 mM glucose for 20 min. Glucagon: perfusion with glucose-free media containing 500 pg/ml glucagon for 2 hrs. The data show a proportional signal intensity.